Biochemical and Biophysical Research Communications 779 (2025) 152459

Contents lists available at ScienceDirect

Biochemical and Biophysical Research Communications

journal homepage: www.elsevier.com/locate/ybbrc

Soluble T-cadherin ameliorates pressure overload-induced heart failure and cardiac fibrosis in mice

Yuta Kondo [a], Shiro Fukuda [a,*], Keitaro Kawada [a], Shunbun Kita [a], Yuto Nakamura [a,1], Hirofumi Nagao [b], Yoshinari Obata [a], Yuya Fujishima [a], Norikazu Maeda [c], Hitoshi Nishizawa [b], Iichiro Shimomura [a]

[a] Department of Metabolic Medicine, Graduate School of Medicine, Osaka University, Osaka, Japan
[b] Department of Metabolism and Atherosclerosis, Graduate School of Medicine, Osaka University, Osaka, Japan
[c] Department of Endocrinology, Metabolism and Diabetes, Faculty of Medicine, Department of Medicine, Kindai University, Osaka, Japan

A B S T R A C T

Aim & objective: We have reported that T-cadherin (T-cad), a glycosylphosphatidylinositol-anchored protein that specifically binds to adiponectin, exists in the human serum as a soluble form (sT-cad). sT-cad promotes pancreatic β-cell proliferations, indicating a potential organ-protective role. This study aimed to the cardioprotective effect of sT-cad.

Methods & results: The sT-cad-expressing plasmid was administered to 7-week-old wild-type mice. One week after administration, transverse aortic constriction (TAC) surgery was performed to induce pressure-overload heart failure. Then, the mice were sacrificed at 2 weeks after the surgery. In the mice that received sT-cad, the TAC-induced increase in heart weight and decline in cardiac function were significantly attenuated. Based on the cardiac histological analysis, sT-cad suppressed both cardiomyocyte hypertrophy and cardiac fibrosis. Cardiac RNA sequencing analysis showed that sT-cad inhibited the TAC-induced upregulation of fibrosis-related genes. In addition, in NIH-3T3 fibroblasts, sT-cad supplementation suppressed the TGF-β-induced mRNA expression of Acta2, a myofibroblast marker.

Conclusion: sT-cad ameliorated the pressure overload-induced heart failure in mice.

1. Introduction

T-cadherin (T-cad), a member of the cadherin family, is unique as it is anchored to the plasma membrane via a glycosylphosphatidylinositol (GPI) moiety and specifically binds to high-molecular-weight adiponectin (HMW-APN), a circulating protein exclusively produced by adipocytes [1–3]. T-cad is predominantly expressed in the heart, skeletal muscle, vascular endothelium, and mesenchymal stem cells [4,5]. Our previous studies have shown that the HMW-APN/T-cad system has protective effects in various organs [4,6–8].

Recently, we reported the existence of T-cad in a soluble form (soluble T-cad). Three distinct forms have been identified: the 130-kDa full-length protein, the 100-kDa form lacking the prodomain, and the 30-kDa prodomain itself. The soluble T-cad exists in a monomer in the human circulation, and it does not bind to HMW-APN [9]. Further, we have reported the effects of soluble T-cad on the pancreas and insulin secretion in mice. The overexpression of soluble T-cad (the 130 kDa full-length protein) in T-cad knockout mice under high-fat diet conditions promoted pancreatic β-cell proliferation [10]. Moreover, the supplementation of recombinant soluble T-cad (without HMW-APN) increased the expression of downstream genes of the Notch signaling pathway in isolated islets from wild-type mice, which pathway is involved in pancreatic β-cell proliferation [10].

While we have reported that (membrane-anchored) T-cad plays a role in mediating the various organ-protective effects of APN. However, recent findings raise the possibility that soluble T-cad itself may exert biological functions on other organs. This study aimed to investigate the cardioprotective effects of soluble T-cad in a heart failure model induced by pressure overload.

* Corresponding author.
E-mail addresses: yuta-kondo@endmet.med.osaka-u.ac.jp (Y. Kondo), s.fukuda@endmet.med.osaka-u.ac.jp (S. Fukuda), k@endmet.med.osaka-u.ac.jp (K. Kawada), shunkita@endmet.med.osaka-u.ac.jp (S. Kita), ynakamura3@bwh.harvard.edu (Y. Nakamura), nagao@endmet.med.osaka-u.ac.jp (H. Nagao), obata-yoshinari@endmet.med.osaka-u.ac.jp (Y. Obata), y.fujishima@endmet.med.osaka-u.ac.jp (Y. Fujishima), norikazu_maeda@med.kindai.ac.jp (N. Maeda), hitoshi1127@endmet.med.osaka-u.ac.jp (H. Nishizawa), ichi@endmet.med.osaka-u.ac.jp (I. Shimomura).
[1] Current address: Kowa Company, Ltd, Tokyo, Japan.

https://doi.org/10.1016/j.bbrc.2025.152459
Received 22 July 2025; Accepted 5 August 2025
Available online 6 August 2025

2. Materials and methods

2.1. Cells, plasmids, chemicals, and reagents

NIH-3T3 fibroblasts were obtained from ATCC and maintained in Dulbecco's Modified Eagle's Medium (DMEM, #16971-55, Nacalai, Japan), supplemented with 10 % fetal bovine serum (#A5256701, Thermo) and 1x Penicillin–Streptomycin Mixed Solution (#26253-84, Nacalai, Japan).

The pLIVE Vector/pLIVE-SEAP Control Vector Kit (#MIR5620) and the TransIT-QR Hydrodynamic Delivery Solution (#MIR5240) were purchased from Mirus Bio. Recombinant human TGF-beta1 (#100-21) was purchased from PeproTech. T-cadherin ELISA kit (#27364–27366) was purchased from Immuno-Biological Laboratories (Japan) (9). The plasmid encoding soluble T-cadherin (pLIVE-sT-cad) was constructed by cloning the coding sequence of the Cdh13 (T-cadherin gene) (NM_019707) without a C-terminal GPI-anchoring site (2079bp) into the pLIVE vector, as previously described [10].

2.2. Animals and experimental procedure: In vivo expression of soluble T-cadherin and the transverse aortic constriction surgery

Male C57BL/6J wild-type mice were obtained from CLEA Japan, Inc. All animal experiments were conducted based on the Guide for the Care and Use of Experimental Animals of Osaka University Graduate School of Medicine (approval no. 03-056-018).

As shown in Fig. 1A, the mice received a single intravenous injection of 10 μg/body of either pLIVE-sT-cad or pLIVE-SEAP plasmid via the tail vein using a hydrodynamic delivery method. Injections were completed within 5 s. No injection-related mortality was observed. One week after plasmid administration, the mice underwent minimal transverse aortic constriction (TAC) or sham surgery, as previously described [4,11]. In brief, the mice were anesthetized with 1.5 % isoflurane. A minimal incision was made, and the aortic arch was constricted with a 7-0 silk suture and a 27G needle, which was subsequently removed. Sham-operated mice underwent a similar procedure without ligation.

Cardiac function was assessed 2 weeks after the surgery using transthoracic echocardiography, as previously described [4], with the LOGIQe ultrasonography system with a 4.0- to 10.0-MHz linear probe (i12L-RS; GE Healthcare). The mice were anesthetized with 1.5 % isoflurane. A two-dimensional guide M-mode trace crossing the ventricular septum and posterior wall was recorded. Ejection fraction was calculated based on the left ventricular internal diameter (LVID) using the Teichholz formula ([7/{2.4 + LVID}] x $LVID^3$). Fractional shortening (FS) was calculated as (end-diastolic LVID - end-systolic LVID)/end-diastolic LVID x 100 (%). After undergoing echocardiography, the mice were sacrificed, and blood and tissue samples were collected for analysis.

2.3. Histological analysis

The apex of the heart was fixed in 10 % neutral-buffered formalin overnight and was then embedded in paraffin. Four-μm thick sections were stained with the Masson's trichrome staining kit (Muto Pure Chemicals Co., Ltd., Japan) for collagen deposition and with wheat germ agglutinin-Alexa Fluor 647 conjugate (#W32466, Thermo) to evaluate cardiomyocyte cross-sectional area (CSA). Image acquisition and quantification were performed using the BZ-x800 microscope and the integrated analysis software (Keyence).

2.4. Preparation of recombinant soluble T-cadherin and cellular experiments

Semi-confluent HEK293 cells were transfected with the pcDNA3.1 plasmid encoding soluble T-cadherin fused with a PA tag (GVAMPGAEDDVV) at the C-terminus for purification. The culture supernatant was subsequently collected, and the soluble T-cadherin was captured by the anti-PA tag antibody beads (#012–25841, FUJIFILM Wako, Japan),

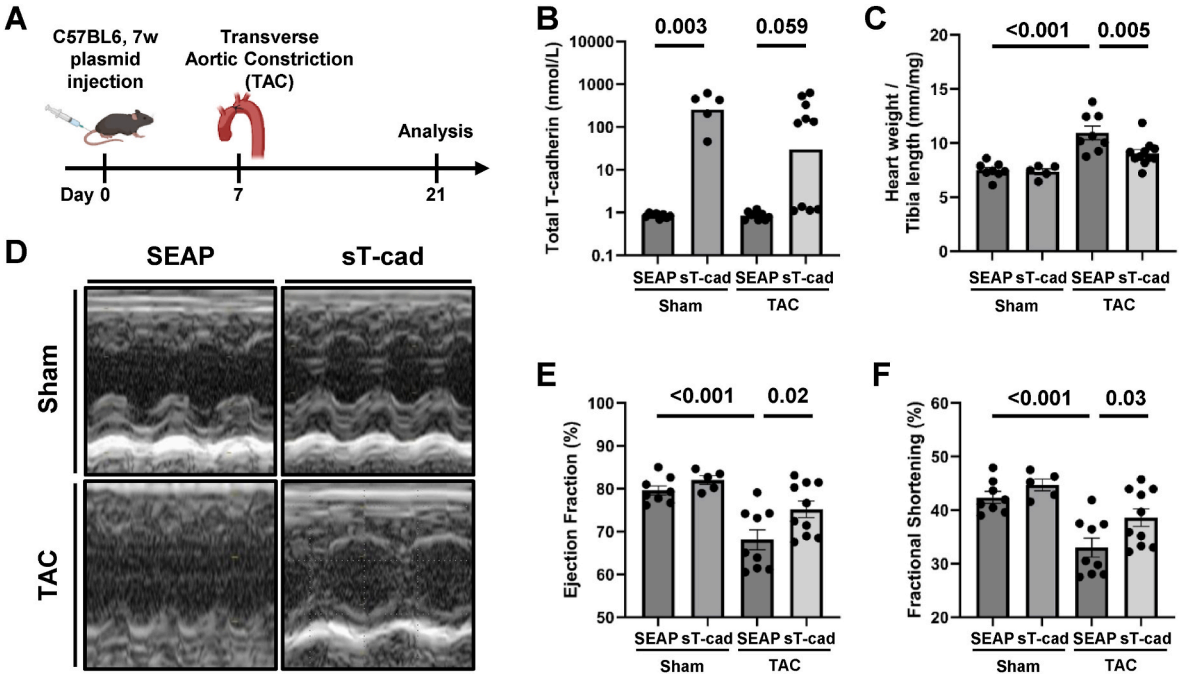

Fig. 1. Soluble T-cadherin (sT-cad) suppressed cardiac dysfunction and heart weight increase induced by the transverse aortic constriction (TAC) surgery. **(A)** Experimental design for the administration of s-T-cad expressing plasmid and the TAC surgery. SEAP (human secreted alkaline phosphatase) was used as the control. **(B)** Plasma total T-cadherin concentrations in each group at 3 weeks after the administration of plasmid (n = 5–10). **(C)** Heart weight per tibia length ratio after the TAC surgery (n = 5–10). **(D)** Representative M-mode images of echocardiography in each group. **(E)** Ejection fraction, and **(F)** fractional shortening after the TAC surgery (n = 5–10). The experiment was conducted three times. Data were presented as the dot plots and means ± standard error. *P*-values are presented above the bar graph. **(B)**: Tukey's test, **(C)–(F)**: One-way analysis of variance with the Dunnett's test (vs the TAC-SEAP group).

according to the manufacturer's instructions. After washing with phosphate-buffered saline (PBS), the captured soluble T-cadherin was eluted with 0.5 M of sodium chloride. The buffer was exchanged into PBS and concentrated using the Amicon Ultra 0.5–100k (#UFC5100BK, Merck Millipore). The purity of the soluble T-cadherin was confirmed as a single band in a sodium dodecyl-sulfate polyacrylamide gel electrophoresis and Coomassie brilliant blue staining.

For the *in vitro* analysis of soluble T-cadherin, NIH-3T3 cells were seeded in 12-well plates at a density of 2.0×10^5 cells/well. After attaching the plate, the medium was changed to serum-free DMEM with 100 nM of soluble T-cadherin. After an overnight serum starvation, the cells were treated with 2 ng/mL of TGF-β and 100 nM of soluble T-cadherin for 24 h.

2.5. Quantitative reverse transcription-polymerase chain reaction and RNA-sequencing

Total RNA was extracted from the heart tissue or NIH-3T3 cells using the TRI Reagent (#T9424, Sigma), according to the manufacturer's instructions. For quantitative reverse transcription-polymerase chain reaction, first-strand cDNA was synthesized using the ReverTra Ace qPCR RT Master Mix (#FSQ-201, Toyobo, Japan). Real-time polymerase chain reaction was performed by QuantStudio7 (Applied Biosystems) with THUNDERBIRD® Next SYBR™ qPCR Mix (#QPX-201, Toyobo, Japan), according to the manufacturer's protocol. The primer sequences were as follows: 36B4 forward, 5- GGCCAATAAGGTGCCAGCT-3 and reverse, 5-TGATCAGCCCGAAGGAGAAG-3; Acta2 forward, 5- GTCCCAGACATCAGGGAGTAA and reverse, 5- TCGGATACTTCAGCGTCAGGA-3.

For RNA-sequencing (RNA-seq), RNA integrity numbers (≥7.0) were confirmed using Agilent Bioanalyzer 2100 (Agilent Technologies). RNA-seq was performed using the NovaSeq 6000 system (Illumina) in the NGS core facility at the Research Institute for Microbial Diseases, the University of Osaka. Expression data were obtained as raw counts and fragments per kilobase of exon per million mapped reads. Differential gene expression analysis was conducted using RNAseqChef version 1.1.4. Differentially expressed genes were defined as genes with a false discovery rate <0.05 and |log2 fold change| ≥ 1.5. The Kyoto Encyclopedia of Genes and Genomes pathway (KEGG pathway) enrichment analysis was conducted to examine the identified gene clusters.

2.6. Statistical analysis

All data were expressed as the means ± standard error. Statistical significance was determined using one-way analysis of variance, followed by the Dunnett's test. P values < 0.05 indicated statistically significant differences. All analyses were performed using the GraphPad Prism 10 software (GraphPad).

3. Results

3.1. Soluble T-cadherin ameliorated TAC-induced heart failure and cardiac hypertrophy

We examined the effect of soluble T-cadherin (soluble T-cad, sT-cad) in a pressure overload-induced heart failure model using transverse aortic constriction (TAC). One week before the TAC surgery, the mice received the pLIVE-vector expressing soluble T-cad (pLIVE-sT-cad). The mice that received the pLIVE-SEAP (expressing human secreted alkaline phosphatase) were used as controls (Fig. 1A).

Two weeks after TAC surgery, the serum concentration of soluble T-cad was increased in the sT-cad group (331 ± 60 nM), compared with that of the control group (0.86 ± 0.03 nM) (Fig. 1B). The TAC surgery resulted in a 1.43-fold increase in heart weight per tibia length ratio (Sham-SEAP: 7.49 ± 0.30 vs TAC-SEAP: 10.8 ± 0.55 mg/mm), which was significantly attenuated by soluble T-cad overexpression (TAC-sT-cad: 9.02 ± 0.46 mg/mm) (Fig. 1C). In addition, soluble T-cad preserved cardiac function by improving both ejection fraction (TAC-SEAP: 68.1 % ± 2.21 % vs TAC-sT-cad: 73.2 % ± 1.78 %) and fractional shortening (TAC-SEAP: 33.0 % ± 1.67 % vs TAC-sT-cad: 36.9 % ± 1.50 %), which were reduced with the TAC surgery (Fig. 1D-F).

3.2. Soluble T-cadherin reduced cardiomyocyte hypertrophy and cardiac fibrosis

To assess cardiac remodeling, the cardiomyocyte cross-sectional area (CSA) was evaluated by the WGA staining, and myocardial fibrosis was quantified using Masson's trichrome staining (Fig. 2). Results showed that soluble T-cad significantly suppressed the TAC-induced increase in the cardiomyocyte CSAs (TAC-SEAP: 241.5 μm^2 vs TAC-sT-cad: 207.0 μm^2) (Fig. 2A and B). Similarly, although the difference did not reach statistical significance, soluble T-cad tended to reduce the extent of fibrotic area caused by the TAC surgery (TAC-SEAP: 3.44 % ± 1.07 % vs TAC-sT-cad: 2.15 % ± 0.18 %) (Fig. 2C and D).

3.3. Soluble T-cadherin altered gene expression related to fibrosis, cardiomyopathy, and mitochondrial function after TAC surgery

Next, to investigate the comprehensive transcriptomic response to soluble T-cad in the heart after the TAC surgery, RNA-seq was performed using cardiac tissue samples collected 2 weeks after the TAC surgery. As shown in Fig. 3A, three clusters of differentially expressed genes (|log2 fold change| ≥ 1.5, false discovery rate <0.05) were identified.

Cluster 1: genes upregulated by TAC and unaffected by soluble T-cad.
Cluster 2: genes upregulated by TAC and downregulated by soluble T-cad.
Cluster 3: genes downregulated by TAC and partially restored by soluble T-cad.

The pathway enrichment analysis revealed the following.

Cluster 1: The focal adhesion and cell adhesion molecules pathways were enriched (Fig. 3B).
Cluster 2: The pathways related to fibrosis (such as extracellular matrix receptor interaction, focal adhesion, and the TGF-β signaling pathway), and cardiac hypertrophy or cardiomyopathy were significantly enriched (Fig. 3C).
Cluster 3: The mitochondrial function pathways (such as oxidative phosphorylation and the TCA cycle, along with various metabolic pathways) were enriched (Fig. 3D).

3.4. Soluble T-cadherin inhibited the TGF-β-induced activation of fibroblasts in vitro

Based on the RNA-seq analysis, various genes were found to be related to fibrosis (such as Col1a1, Col3a1, and FN1) and TGF-β signaling (such as Tgfb1, Gdf6, and Id3), which upregulated by TAC and downregulated by soluble T-cad, enriched in the Cluster 2 (Fig. 4A). Considering the important role of TGF-β signaling in cardiac fibrosis and fibroblast activation into myofibroblasts [12–14], we assessed the effect of soluble T-cad on TGF-β-induced gene expression in NIH-3T3 fibroblasts.

The cells were pretreated with recombinant soluble T-cad (100 nmol/L) overnight and then co-treated with TGF-β (2 ng/mL) for 24 h (Fig. 4B). Soluble T-cad did not significantly suppress the TGF-β-induced expression of Col1a1 (TGF-β: 1.43 ± 0.05-fold vs TGF-β + sT-cad: 1.38 ± 0.02-fold) (Fig. 4C). However, soluble T-cad significantly reduced the expression of Acta2 (TGF-β: 7.07 ± 0.27-fold vs TGF-β + sT-cad: 5.66 ± 0.26-fold), a marker of myofibroblast activation (Fig. 4D).

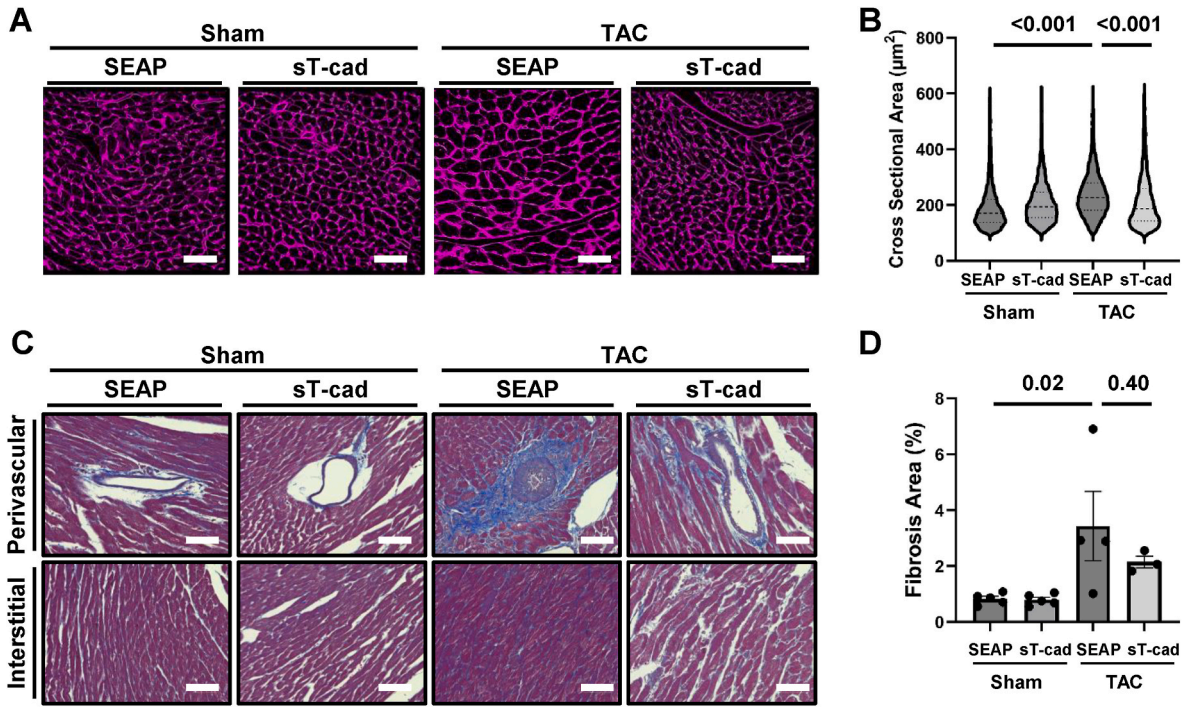

Fig. 2. Soluble T-cadherin (sT-cad) suppressed cardiac hypertrophy and cardiac fibrosis induced by the transverse aortic constriction (TAC) surgery. **(A)** Representative images of the heart sections stained with wheat-germ agglutinin in each group after the TAC surgery, as shown in Fig. 1. The scale bar indicates 50 μm. **(B)** Quantification of the cardiomyocyte cross-sectional area after the TAC surgery (20–25 fields per individual). **(C)** The representative images of the heart sections (perivascular lesions and interstitial lesions of the heart) were analyzed via Masson's trichrome staining in each group after the TAC surgery. The scale bar indicates 50 μm. **(D)** Quantification of the fibrotic area after the TAC surgery (5 fields per section). Data were presented as the dot plots and means ± standard error. *P*-values are presented above the bar graph. One-way analysis of variance with the Dunnett's test (vs the TAC-SEAP group).

4. Discussion

In this study, we demonstrated that soluble T-cadherin (soluble T-cad) suppressed cardiac dysfunction in the TAC model (Figs. 1 and 2), in part by suppressing cardiac fibrosis (Figs. 3 and 4). Heart failure is the major cause of mortality and morbidity. Although various therapeutic strategies are available, approaches that can inhibit the pathogenic mechanisms of heart failure are limited. To the best of our knowledge, this study first reported that the overexpression of a soluble protein in organs (liver) other than the heart rescued cardiac dysfunction in a pressure overload-induced heart failure model.

We previously reported that soluble T-cad regulates pancreatic β-cell proliferation via the Notch signaling pathway [10]. Notch signaling also plays an important role in regulating cardiac fibroblasts and cardiac fibrosis [15]. For example, Nemir et al. showed that transgenic mice overexpressing the Notch1 ligand Jagged1 on the surface of cardiomyocytes exhibited decreased cardiac fibrosis after the TAC surgery, thereby showing that Notch activation is a protective mechanism in the cardiac fibrosis [16]. That is why we investigated cardiac effects of soluble T-cad in this study. However, in the current RNA-seq analysis of the heart tissue samples, soluble T-cad did not significantly alter the expression of Notch target genes (such as HES1, HEY1, and HEY2 (**data not shown**)). Thus, we hypothesized that soluble T-cad engages distinct signaling pathways depending on the tissue.

Transverse aortic constriction (TAC) surgery is a well-established animal model for examining cardiac fibrosis and hypertrophy. Several studies have revealed the essential role of TGF-β signaling in mediating cardiac fibrosis and hypertrophy after pressure overload [13,14]. TGF-β contributes to cardiac remodeling via autocrine and paracrine mechanisms [13] and regulates the transition of cardiac fibroblasts into activated myofibroblasts [17]. We investigated the mechanism of the soluble T-cad in the TAC model, and found the alteration in the expression of genes related to fibrosis and the TGF-β signaling pathways in the RNA-seq of the heart (Figs. 3C and 4A), both of which were suppressed by the soluble T-cad. Indeed, the supplementation of soluble T-cad to NIH-3T3 fibroblasts suppressed the expression of Acta2, a well-known marker of myofibroblast activation (Fig. 4D), suggesting that soluble T-cad partially interferes with the TGF-β–driven transition to myofibroblast.

T-cadherin is a unique member of the cadherin superfamily, anchored to the plasma membrane via a GPI moiety, and is a specific and physiological binding partner of adiponectin [1,3,18]. However, our previous gel filtration analysis has shown that soluble T-cad exists as a monomer in the serum and is does not form stable complexes with adiponectin [9]. Based on the current *in vitro* findings (Fig. 4), soluble T-cad, independent of adiponectin, directly suppressed TGF-β signaling in the fibroblasts. Since the molecular weight of soluble T-cad used in this study is approximately 130 kDa, the likely receptor for soluble T-cad is located on the cell surface rather than intracellularly. Although RNA-seq analysis showed that the mitochondrial function improved with soluble T-cad treatment (Fig. 3D), this is likely a secondary effect caused by improved cardiac function rather than a direct mitochondrial action of soluble T-cad.

Considering that the concentrations were >100-fold higher than the physiological levels in this study, the observed effects may reflect pharmacological actions rather than physiological ones. Nevertheless, soluble T-cad had minimal impact on gene expression in the hearts of sham-operated mice (Fig. 3), suggesting that soluble T-cad may become functionally active at the time of cardiac stress or injury. While further studies to elucidate the molecular mechanism of cardioprotective effect and the regulation of soluble T-cad synthesis *in vivo* are needed, soluble T-cad may become a therapeutic target for heart failure.

CRediT authorship contribution statement

Yuta Kondo: Conceptualization, Data curation, Investigation,

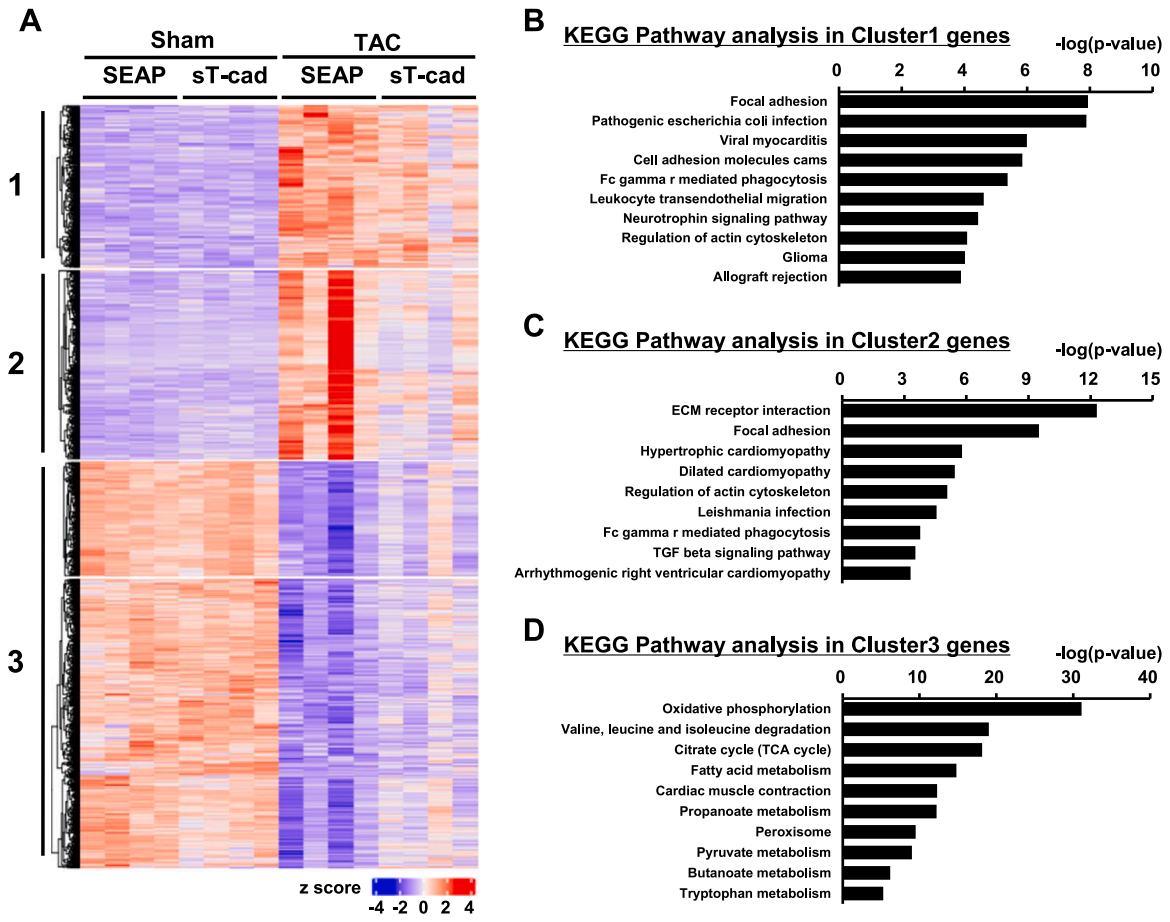

Fig. 3. RNA-sequencing analysis of the heart with or without soluble T-cadherin (sT-cad) administration.
(A) Heatmap based on z-scores and the cluster analysis of differentially expressed genes (DEGs) in each group (fold ≥1.5). **(B–D)** The KEGG pathway analyses of DEGs were performed in **(B)** cluster 1 (upregulated by the transverse aortic constriction (TAC) surgery and not changed by sT-cad), **(C)** cluster 2 (upregulated by the TAC surgery and downregulated by sT-cad), and **(D)** cluster 3 (downregulated by the TAC surgery and upregulated by sT-cad).

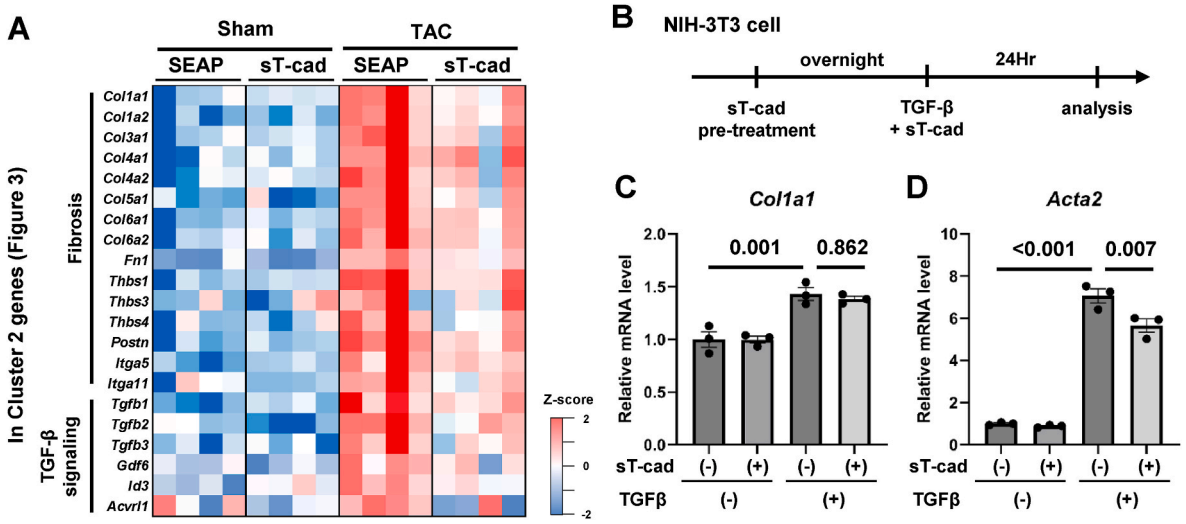

Fig. 4. Soluble T-cadherin (sT-cad) suppressed the Acta2 upregulation by TGF-β in the NIH-3T3 fibroblasts.
(A) Heatmap of the mRNA expression associated with fibrosis and TGF-β signaling in the cluster 2 (Fig. 3C). **(B)** Experimental design. The NIH-3T3 cells were incubated with recombinant soluble T-cadherin (100 nmol/L) overnight. After pre-treatment, the cells were incubated with TGF-β (2 ng/mL) and soluble T-cadherin (100 nmol/L). **(C–D)** Quantitative PCR analysis of the **(C)** Col1a1 and **(D)** Acta2 mRNA expression of NIH-3T3 cells after co-incubation with TGF-β and sT-cad (n = 3 in each group). Each expression was normalized by the 36B4 expression. The experiment was conducted two times. Data were presented as the dot plots and means ± standard error. *P*-values are presented above the bar graph. One-way analysis of variance with the Dunnett's test (vs the TGFβ(+)sT-cad(−) group).

Methodology, Visualization, Writing – original draft. **Shiro Fukuda:** Conceptualization, Data curation, Formal analysis, Funding acquisition, Investigation, Methodology, Project administration, Validation, Visualization, Writing – original draft, Writing – review & editing. **Keitaro Kawada:** Data curation, Investigation, Methodology, Validation. **Shunbun Kita:** Conceptualization, Formal analysis, Funding acquisition, Supervision, Writing – review & editing. **Yuto Nakamura:** Conceptualization, Investigation, Methodology, Validation, Writing – review & editing. **Hirofumi Nagao:** Funding acquisition, Writing – review & editing. **Yoshinari Obata:** Writing – review & editing. **Yuya Fujishima:** Funding acquisition, Writing – review & editing. **Norikazu Maeda:** Funding acquisition, Writing – review & editing, Supervision. **Hitoshi Nishizawa:** Funding acquisition, Supervision, Writing – review & editing. **Iichiro Shimomura:** Funding acquisition, Supervision, Writing – review & editing.

Data and code availability

- RNA-seq datasets were deposited in NCBI under accession number GSE301839.
- This paper does not report the original code.
- Any additional information required to reanalyse the data reported in this paper is available from the lead contact upon request.

Funding

This work was supported by Grants-in-Aid for Scientific Research [23K07989 to NM, 23K08006 to HNi, 24K02504 to IS, 24K11675 to YF], Grants-in-Aid for Early Career Scientists [24K19289 to SF, 24K19305 to HNa], AMED-CREST [to IS], Grants from the Manpei Suzuki Diabetes Foundation [to SF, to HNa], Lotte Research Promotion Grant (to HNa), the MSD Life Science Foundation, Public Interest Incorporated Foundation [to SF, to HNa], Japan Diabetes Society Junior Scientist Development Grant supported by Novo Nordisk Pharma Ltd. [to SF], Research Grants from Kowa Life Science Foundation [to SF], Joint Research Grants with Kowa Pharmaceutical [to IS], and Uehara Memorial Foundation [to IS]. The funding agencies had no role in the study design, data collection and analysis, decision to publish, or preparation of the article.

Declaration of competing interest

The authors declare the following financial interests/personal relationships which may be considered as potential competing interests: Yuto Nakamura reports a relationship with Kowa Co Ltd that includes: employment. If there are other authors, they declare that they have no known competing financial interests or personal relationships that could have appeared to influence the work reported in this paper.

Acknowledgements

We acknowledge the NGS core facility at the Research Institute for Microbial Diseases of the University of Osaka for the sequencing and data analysis. We thank the staff at the Center of Medical Research and Education (CentMeRE) in Graduate School of Medicine of the University of Osaka, for excellent technical support and assistance, as well as all members of the Third Laboratory (Adiposcience Laboratory), Department of Metabolic Medicine, Osaka University, for helpful discussion of the project.

References

[1] S. Kita, S. Fukuda, N. Maeda, I. Shimomura, Native adiponectin in serum binds to mammalian cells expressing T-cadherin, but not AdipoRs or calreticulin, eLife 8 (2019 Oct) e48675.
[2] B. Ranscht, M.T. Dours-Zimmermann, T-cadherin, a novel cadherin cell adhesion molecule in the nervous system lacks the conserved cytoplasmic region, Neuron 7 (3) (1991 Sep) 391–402.
[3] S. Fukuda, S. Kita, Y. Obata, Y. Fujishima, H. Nagao, S. Masuda, et al., The unique prodomain of T-cadherin plays a key role in adiponectin binding with the essential extracellular cadherin repeats 1 and 2, J. Biol. Chem. 292 (19) (2017 May) 7840–7849.
[4] Y. Nakamura, S. Kita, Y. Tanaka, S. Fukuda, Y. Obata, T. Okita, et al., Adiponectin stimulates exosome release to enhance mesenchymal stem-cell-driven therapy of heart failure in mice, Mol. Ther. 28 (10) (2020 Oct) 2203–2219.
[5] K. Matsuda, Y. Fujishima, N. Maeda, T. Mori, A. Hirata, R. Sekimoto, et al., Positive feedback regulation between adiponectin and T-Cadherin impacts adiponectin levels in tissue and plasma of Male mice, Endocrinology 156 (3) (2015 Mar 1) 934–946.
[6] Y. Tsugawa-Shimizu, Y. Fujishima, S. Kita, S. Minami, T aki Sakaue, Y. Nakamura, et al., Increased vascular permeability and severe renal tubular damage after ischemia-reperfusion injury in mice lacking adiponectin or T-cadherin, Am. J. Physiol. Endocrinol. Metabol. 320 (2) (2021 Feb 1) E179–E190.
[7] Y. Fujishima, N. Maeda, K. Matsuda, S. Masuda, T. Mori, S. Fukuda, et al., Adiponectin association with T-cadherin protects against neointima proliferation and atherosclerosis, FASEB J. 31 (4) (2017 Apr) 1571–1583.
[8] Y. Tanaka, S. Kita, H. Nishizawa, S. Fukuda, Y. Fujishima, Y. Obata, et al., Adiponectin promotes muscle regeneration through binding to T-cadherin, Sci. Rep. 9 (1) (2019 Jan) 16.
[9] S. Fukuda, S. Kita, K. Miyashita, M. Iioka, J. Murai, T. Nakamura, et al., Identification and clinical associations of 3 forms of circulating T-cadherin in human serum, J. Clin. Endocrinol. Metab. 106 (5) (2021 Apr) 1333–1344.
[10] T. Okita, S. Kita, S. Fukuda, K. Fukuoka, E. Kawada-Horitani, M. Iioka, et al., Soluble T-cadherin promotes pancreatic β-cell proliferation by upregulating Notch signaling, iScience 25 (11) (2022 Nov) 105404.
[11] T.P. Martin, E. Robinson, A.P. Harvey, M. MacDonald, D.J. Grieve, A. Paul, et al., Surgical optimization and characterization of a minimally invasive aortic banding procedure to induce cardiac hypertrophy in mice, Exp. Physiol. 97 (7) (2012 Jul) 822–832.
[12] H. Khalil, O. Kanisicak, V. Prasad, R.N. Correll, X. Fu, T. Schips, et al., Fibroblast-specific TGF-β–Smad2/3 signaling underlies cardiac fibrosis, J. Clin. Investig. 127 (10) (2017 Sep 11) 3770–3783.
[13] A.V. Villar, M. Cobo, M. Llano, C. Montalvo, F. González-Vílchez, R. Martín-Durán, et al., Plasma levels of transforming growth Factor-β1 reflect left ventricular remodeling in aortic stenosis, in: A. Leri (Ed.), Plos ONE, vol. 4, 2009 Dec 30 e8476, 12.
[14] N.G. Frangogiannis, Transforming growth factor-β in myocardial disease, Nat. Rev. Cardiol. 19 (7) (2022 Jul) 435–455.
[15] P. Docshin, D. Panshin, A. Malashicheva, Molecular interplay in cardiac fibrosis: exploring the functions of RUNX2, BMP2, and notch, Rev. Cardiovasc. Med. 25 (10) (2024 Oct 16) 368.
[16] M. Nemir, M. Metrich, I. Plaisance, M. Lepore, S. Cruchet, C. Berthonneche, et al., The Notch pathway controls fibrotic and regenerative repair in the adult heart, Eur. Heart J. 35 (32) (2014 Aug 21) 2174–2185.
[17] L. Hortells, A.K.Z. Johansen, K.E. Yutzey, Cardiac fibroblasts and the extracellular matrix in regenerative and nonregenerative hearts, JCDD 6 (3) (2019 Aug 20) 29.
[18] C. Hug, J. Wang, N.S. Ahmad, J.S. Bogan, T.S. Tsao, H.F. Lodish, T-cadherin is a receptor for hexameric and high-molecular-weight forms of Acrp30/adiponectin, Proc. Natl. Acad. Sci. USA. 101 (28) (2004 Jul 13) 10308–10313.